Available online at www.sciencedirect.com

ScienceDirect

www.elsevier.com/locate/jes

JES JOURNAL OF ENVIRONMENTAL SCIENCES www.jesc.ac.cn

Complex interplay between formation routes and natural organic matter modification controls capabilities of C_{60} nanoparticles (nC_{60}) to accumulate organic contaminants

Lei Hou[1,2], *John D. Fortner*[3], *Ximeng Wang*[2], *Chengdong Zhang*[2], *Lilin Wang*[2], *Wei Chen*[2,*]

1. *College of Environmental Science and Engineering, Southwest Forestry University, Kunming 650224, China. E-mail: houlei_1985@126.com*
2. *College of Environmental Science and Engineering, Nankai University, Tianjin 300071, China*
3. *Department of Energy, Environmental and Chemical Engineering, Washington University in St. Louis, MO 63130, USA*

ARTICLE INFO

Article history:
Received 7 April 2016
Revised 24 July 2016
Accepted 29 July 2016
Available online 11 August 2016

Keywords:
Fullerene nanoparticles
Aggregation
Natural organic matter
Organic contaminants
Adsorption

ABSTRACT

Accumulation of organic contaminants on fullerene nanoparticles (nC_{60}) may significantly affect the risks of C_{60} in the environment. The objective of this study was to further understand how the interplay of nC_{60} formation routes and humic acid modification affects contaminant adsorption of nC_{60}. Specifically, adsorption of 1,2,4,5-tetrachlorobenzene (a model nonionic, hydrophobic organic contaminant) on nC_{60} was greatly affected by nC_{60} formation route – the formation route significantly affected the aggregation properties of nC_{60}, thus affecting the available surface area and the extent of adsorption *via* the pore-filling mechanism. Depending on whether nC_{60} was formed *via* the "top-down" route (*i.e.*, sonicating C_{60} powder in aqueous solution) or "bottom-up" route (*i.e.*, phase transfer from an organic solvent) and the type of solvent involved (toluene *versus* tetrahydrofuran), modification of nC_{60} with Suwannee River humic acid (SRHA) could either enhance or inhibit the adsorption affinity of nC_{60}. The net effect depended on the specific way in which SRHA interacted with C_{60} monomers and/or C_{60} aggregates of different sizes and morphology, which determined the relative importance of enhanced adsorption from SRHA modification *via* preventing C_{60} aggregation and inhibited adsorption through blocking available adsorption sites. The findings further demonstrate the complex mechanisms controlling interactions between nC_{60} and organic contaminants, and may have significant implications for the life-cycle analysis and risk assessment of C_{60}.

Introduction

Buckminster fullerene (C_{60}) is an important carbon nanomaterial that has great potential in various fields such as cancer therapeutics, drug delivery, and computer sensors (Simon et al., 2007; Campoy-Quiles et al., 2008; Li et al., 2008; Mauter and Elimelech, 2008). With the increasing production and use of this material, its environmental release is inevitable (Klaine et al., 2008). The potential risks of C_{60}, in particular, colloidal nano-scale C_{60} aggregates (*i.e.*, nC_{60}), have received considerable attention, with a number of studies demonstrating C_{60} toxicity (Sayes et al., 2004; Klaine et al., 2008). Further, in natural environments C_{60} can accumulate organic contaminants (Yang et al., 2006; Gai et al., 2011; Zhang et al., 2011), which may further alter the risk profiles (Henry et al., 2007).

* *Corresponding author*. E-mail: chenwei@nankai.edu.cn (Wei Chen).

http://dx.doi.org/10.1016/j.jes.2016.07.009
1001-0742/

To date, only limited studies have examined the adsorptive interactions between C_{60} and common organic contaminants (including naphthalene, phenanthrene, fluoranthene, pyrene, chrysene, 1,2-dichlorobenzene, and atrazine), and the results show that the adsorption affinities of C_{60} are strongly dependent on its aggregation properties (Cheng et al., 2004, 2005; Yang et al., 2006; Yang and Xing, 2007; Hu et al., 2008; Gai et al., 2011; Hüffer et al., 2013). For example, Cheng et al. (2004) reported that small C_{60} aggregates with diameters of 1–3 μm (formed by magnetically stirring C_{60} powder in a solution containing 0.01 mol/L NaCl and 0.01 mol/L NaN_3) exhibited much stronger adsorption affinity for naphthalene than did large C_{60} aggregates with diameters of 20–50 μm, likely due to the increased number of adsorption sites per unit of C_{60} (aggregate) mass for the smaller aggregates. Similarly, Gai et al. (2011) reported that adsorption affinities of C_{60} aggregates (0.14–15.28 μm) increased with decreasing particle size. Interestingly, in another study by Cheng et al. (2005), it was found that an nC_{60} sample prepared by solvent exchange from toluene had lower adsorption affinity for naphthalene than small aggregates formed simply through physical mixing. Gai et al. (2011) also made very similar observations using atrazine, and attributed the lower adsorption nC_{60} to its lower pore volume. Thus, it appears that the formation routes/mechanisms of nC_{60} (and subsequent aggregation processes) play a critical role in the adsorption affinities of the aggregates.

Chang et al. (2012) categorized the formation mechanisms of nC_{60} into two general routes as (1) top-down routes whereby nC_{60} is formed by breaking large aggregates into smaller ones (*e.g.*, physically mixing C_{60} powder in aqueous solutions), and (2) bottom-up approaches whereby nC_{60} forms from a seed-growth mechanism (solvent exchanging C_{60} from organic solvent to aqueous solution). In general, nC_{60} formed through top-down routes is typically larger in size and irregularly shaped (Duncan et al., 2008; Chang and Vikesland, 2009), whereas nC_{60} formed *via* the bottom-up route is smaller in size with more ordered, crystalline structures (Brant et al., 2005, 2006; Fortner et al., 2005). Further, nC_{60} samples formed *via* solvent exchange methods can vary significantly depending on the specific solvents used (Brant et al., 2006; Xie et al., 2008). To date, little is known about how formation routes of nC_{60} fundamentally affect the adsorption affinities toward common organic contaminants.

It has been demonstrated that natural organic matter (NOM) can significantly affect the adsorption properties of nC_{60} (Hu et al., 2008; Gai et al., 2011). Adsorption of NOM to C_{60} aggregates can cover (or effectively block) available adsorption sites or pores of C_{60} aggregates, thus inhibiting adsorption (Hu et al., 2008; Gai et al., 2011). NOM can also enhance the dispersion of C_{60} (Xie et al., 2008; Li et al., 2009; Qu et al., 2010), consequently rendering more available adsorption sites. Gai et al. (2011) found that nC_{60} aggregates formed by stirring C_{60} powder in a humic acid (HA) solution had greater adsorption affinity for atrazine than nC_{60} formed in the absence of HA, and the specific enhancement extent depended on how much enhanced dispersion due to HA modification counterbalanced the pore-blocking effect of HA. Taken together, we hypothesize that the specific effects of NOM modification on the adsorption affinities of nC_{60} will also largely depend on the formation routes of nC_{60}.

The objective of this study was to understand how the complex interplay between formation routes and NOM modification can affect the adsorption affinity of nC_{60} for organic contaminants. One physical mixing (sonication) and two solvent exchange (toluene *vs.* tetrahydrofuran (THF)) approaches were chosen to prepare nC_{60} samples, and NOM modification was performed with Suwannee River humic acid (SRHA) during or after the formation of nC_{60}. A nonionic, hydrophobic organic molecule, 1,2,4,5-tetrachlorobenzene (TeCB), was selected as a model organic compound to avoid potential complications such as polar and electrostatic interactions. The combined effects of formation routes and SRHA modification were analyzed based on the physicochemical properties of the nC_{60} samples and their adsorption affinities for TeCB.

1. Materials and methods

1.1. Materials and chemicals

Pristine fullerene powder (C_{60}, >99.5%) was purchased from SES Research (USA). SRHA was obtained from the International Humic Substances Society (USA), and is reported to be composed of 52.63 wt% carbon, 4.28 wt% hydrogen, 42.04 wt% oxygen, and a small amount of nitrogen, sulfur, and phosphate; the distribution of functional groups is: carboxylic (21%), aromatic (31%), aliphatic (29%), and heteroaliphatic (20%). Glass optical fibers with a 30-μm polydimethylsiloxane coating were purchased from Polymicro Technologies (USA). The fibers were cut into 3 cm lengths, and cleaned three times with 1:1 (v:v) methanol/water by shaking, then washed with deionized (DI) water to remove all the solvent, and stored in DI water until further use. 1,2,4,5-Tetrachlorobenzene (TeCB, >99%), chromatographic grade toluene and THF were purchased from Sigma Aldrich (USA).

1.2. Preparation and characterization of nC_{60} samples

The nC_{60} samples were prepared using two solvent exchange methods and a physical mixing method. The solvent exchange method using toluene was similar to that reported by Andrievsky et al. (1995). Briefly, 20 mL of a C_{60} solution (1 g/L in toluene) was added to 200 mL of a 0.5 mmol/L NaCl solution and sonicated with a probe (Vibra-Cell VCX800, Sonics & Material Inc., USA) at 100 W for 3 hr in the dark. The yellow-colored suspension generated was first filtered with a 1-μm glass membrane filter and then with a 0.45-μm cellulose acetate membrane filter (Millipore Co., USA) to remove large C_{60} aggregates. The nC_{60} samples prepared using this method are referred to as "TOL-nC_{60}".

The method developed by Fortner et al. (2005) was used to prepare nC_{60} samples from C_{60} in THF. Briefly, 200 mL of a C_{60} solution (~9 mg/L in THF) was added to a 2-L flask and stirred rapidly. Then, 200 mL of a 0.5 mmol/L NaCl solution was added at a rate of 500 mL/min to obtain a transparent yellowish suspension. Then the suspension was heated at 75–80°C using a rotary evaporator (RE-501, Hongguan Instrument Co., CN) to remove THF. To ensure a consistent level of THF removal from solution, a stepwise evaporating procedure was used as follows (Fortner et al., 2005). Starting with 400 mL

total volume (1:1 (v:v), water:THF), 220 mL was evaporated and collected. The remaining yellow solution was diluted with 40 mL of 0.5 mmol/L NaCl solution. The solution was then evaporated again to 180 mL and then diluted with 40 mL of 0.5 mmol/L NaCl solution. Finally, the solution was evaporated again to the final volume of 200 mL. Afterward, the nC_{60} suspension was filtered with a 0.45 μm cellulose acetate membrane filter to remove large C_{60} aggregates. The nC_{60} samples prepared using this method are referred to as "THF-nC_{60}".

For the physical mixing method, which is similar to that reported by Hwang and Li (2010), a mixture of 100 mg C_{60} powder and 200 mL 0.5 mmol/L NaCl solution was sonicated at 100 W using the abovementioned sonication probe for 2 hr. Then, the suspension was filtered with 1-μm glass membrane filters. The nC_{60} samples prepared using this method are referred to as "SON-nC_{60}".

For each preparation method, two SRHA-modified samples were prepared. The first set of SRHA-modified samples (indicated by a suffix "/SRHA", *i.e.*, "TOL-nC_{60}/SRHA", "THF-nC_{60}/SRHA" and "SON-nC_{60}/SRHA") were obtained by replacing the 200 mL 0.5 mmol/L NaCl solution with a 5 mg/L SRHA solution. To prepare the second set of SRHA-modified samples (indicated by a suffix "+SRHA", *i.e.*, "TOL-nC_{60} + SRHA", "THF-nC_{60} + SRHA" and "SON-nC_{60} + SRHA"), the nC_{60} samples made in the absence of SRHA were equilibrated with a SRHA solution by magnetically stirring for 4 hr in the dark, to give a final concentration of SRHA of approximately 5 mg/L. All the SRHA-modified nC_{60} samples were dialyzed using dialysis bags of 6000–8000 molecular weight cutoff to remove the freely dissolved SRHA (Li et al., 2009). All the nC_{60} samples were kept in the dark at 4°C and were stable during the period of this research. The concentrations of C_{60} in the nC_{60} samples were determined using an oxidation–toluene extraction procedure (Fortner et al., 2005). The presence of a small amount of HA (below 5 mg/L) in the solution had negligible effect on the C_{60} measurement (Xie et al., 2008). The ultraviolet (UV) absorbance spectra of the nC_{60} samples were recorded with a UV/vis spectrophotometer (TU1810, Puxi Instruments Co., CN). The scan was performed in the wavelength range of 200–600 nm. The slit width and sample interval were set at 1 and 0.2 nm, respectively. Hydrodynamic diameters (Z_{ave}) and particle size distributions of the nC_{60} samples were measured by dynamic light scattering (DLS) and ζ potentials were measured by electrophoretic mobility at 25°C using a ZetaPALS (Brookhaven Instruments, USA). The morphology of all nC_{60} samples was examined with a transmission electron microscope (TEM, JEM-2100, JEOL, Japan) operated at 80 kV. The samples were prepared by air-drying a drop of each nC_{60} sample onto a copper TEM grid (Electron Microscopy Sciences, USA).

1.3. Adsorption experiments

Prior to initiating an adsorption experiment, a series of brown amber glass vials each containing 20 mL nC_{60} suspension were prepared. Then, different amounts of TeCB stock solution (in methanol) was added to the vials. The vials were capped and tumbled end-over-end at 1 r/min for 5 days to reach adsorption equilibrium. Afterward, fibers were exposed to the nC_{60} suspensions and were allowed to equilibrate for another 5 days (see the sorption kinetics in Appendix A, Fig. S1). Then, the fibers were taken out, wiped with a wet tissue, and extracted with hexane to analyze the concentrations of TeCB on the fibers. The concentrations of freely dissolved TeCB were calculated based on the concentrations on the fibers and the distribution coefficient of TeCB to the fiber (the procedures used to determine the fiber–water distribution coefficient are given in Appendix A). The concentrations of TeCB on nC_{60} were calculated based on mass balance. All the samples were run in duplicate. The blank control samples of TeCB showed no degradation during the adsorption experiments, and pH remained constant during all the experiments. The adsorption affinity of TeCB on SRHA was also tested using the procedures mentioned above, and the only difference was that the nC_{60} suspension was replaced with 5 mg/L SRHA solution.

The concentrations of TeCB were determined using a gas chromatograph equipped with an electron capture detector (6890N, Agilent, USA) and an HP-5 capillary column. No peaks for potential degradation or transformation products were detected in the spectra.

2. Results and discussion

2.1. Characteristics of nC_{60} samples

Physicochemical properties of the nine nC_{60} samples are summarized in Table 1. The results indicate that the aggregation properties and surface charge of nC_{60} are greatly dependent on the synthesis route by which nC_{60} was formed. The nC_{60} samples prepared through solvent exchange methods were considerably smaller in size compared with the nC_{60} samples prepared *via* physical mixing (Fig. 1): the Z_{ave} values of the three nC_{60} samples prepared by sonication ranged from 303.5 to 350.2 nm, whereas the Z_{ave} values of the six samples prepared by solvent exchange were only 124.2 to 173.8 nm. Furthermore, nC_{60} samples made using the two different solvent exchange methods also differed considerably in size and uniformity — samples made through THF exchange were smaller and more uniform in size, as indicated by having the smallest polydispersity index values. The morphological differences among the nC_{60} samples formed *via* these different routes are evident from the TEM micrographs (Fig. 2). The samples synthesized through physical mixing were irregular in shape. In comparison, the samples made by solvent exchange from toluene were generally spherical, which was in contrast to the samples synthesized through solvent exchange *via* THF, which were in ordered (faceted) crystalline forms. Morphological differences shown in Fig. 2 are also consistent with the findings in the literature (Fortner et al., 2005; Brant et al., 2006; Duncan et al., 2008; Xie et al., 2008; Gai et al., 2011; Chang et al., 2012; Wang et al., 2014). Compared with the aggregates formed *via* "top-down" routes (*e.g.*, sonication as used in this study), by which large C_{60} aggregates are broken into smaller ones, the aggregates formed *via* "bottom-up" routes (*e.g.*, solvent exchange) are built from monomers or crystalline primary aggregates (Andrievsky et al., 2002; Avdeev et al., 2004; Brant et al., 2006; Chen and Elimelech, 2006). Thus, it is likely that the aggregates formed *via* solvent exchange are more orderly and tightly packed, especially for the case of solvent exchange with THF.

Table 1 – Summary of physicochemical properties and adsorption parameters (K_F and n of Freundlich model and distribution coefficients K_d) of different nC_{60} samples.

Sample ID	Physicochemical properties				Fitted adsorption parameters			
	ζ potential (mV)	Z_{ave} (nm)	PDI	λ_{max} (nm)	K_F ($(L^n \cdot mmol^{1-n})/kg$)	n	R^2	Log K_d (L/kg)
SON- nC_{60}	−26.01	350.2	0.195	355	1130 ± 767	0.543 ± 0.108	0.862	4.08–5.16
SON-nC_{60}/SRHA	−23.84	303.5	0.217	354	2820 ± 714	0.493 ± 0.036	0.983	4.85–5.60
SON-nC_{60} + SRHA	−27.77	315.1	0.092	353	2140 ± 433	0.522 ± 0.029	0.989	4.64–5.33
TOL- nC_{60}	−16.40	160.2	0.164	342	4870 ± 598	0.558 ± 0.019	0.996	4.82–5.68
TOL-nC_{60}/SRHA	−23.39	124.2	0.268	342	3440 ± 745	0.472 ± 0.034	0.978	4.84–5.82
TOL-nC_{60} + SRHA	−22.40	151.4	0.156	341	6260 ± 3000	0.669 ± 0.078	0.952	4.61–5.53
THF- nC_{60}	−22.78	173.8	0.005	344	197,000 ± 121,000	1.054 ± 0.094	0.974	4.88–5.22
THF-nC_{60}/SRHA	−35.01	164.8	0.012	345	32,900 ± 3450	0.935 ± 0.017	0.999	4.37–4.79
THF-nC_{60} + SRHA	−24.28	167.7	0.005	344	196,000 ± 94,900	1.109 ± 0.076	0.985	4.81–5.04

PDI: polydispersity index.

The effects of SRHA modification on the aggregation properties of the nC_{60} samples were also dependent on the formation route (Table 1 and Fig. 2). For the samples prepared through physical mixing, SRHA modification significantly decreased particle size (Z_{ave}) both when SRHA was present during the sonication and when added afterward. When sonicating C_{60} powder in SRHA solution, SRHA could stabilize the small C_{60} aggregates taken apart by physical forces and thus prevent them from aggregating again. The fact that when SRHA was added after sonication the sizes of C_{60} aggregates were still substantially decreased indicates that the packing of C_{60} aggregates formed by sonication was relatively loose in nature, and could be broken down into smaller pieces under appropriate energy conditions. For samples prepared by solvent exchange with toluene, significant reduction in particle size (Z_{ave}) was only observed when SRHA was present during the formation of nC_{60}. This was expected, as C_{60} aggregates formed *via* this route were tightly packed and not easily broken down. For the samples prepared by solvent exchange with THF, SRHA modification only slightly decreased the Z_{ave}, regardless of the stage in which SRHA was introduced. This was likely because the dispersing effect of SRHA was relatively small, owing to the water miscibility of THF. The preparation-method-dependent effects of SRHA modification on size distribution of nC_{60} are generally consistent with results in the literature (Xie et al., 2008; Wang et al., 2012, 2014). The TEM

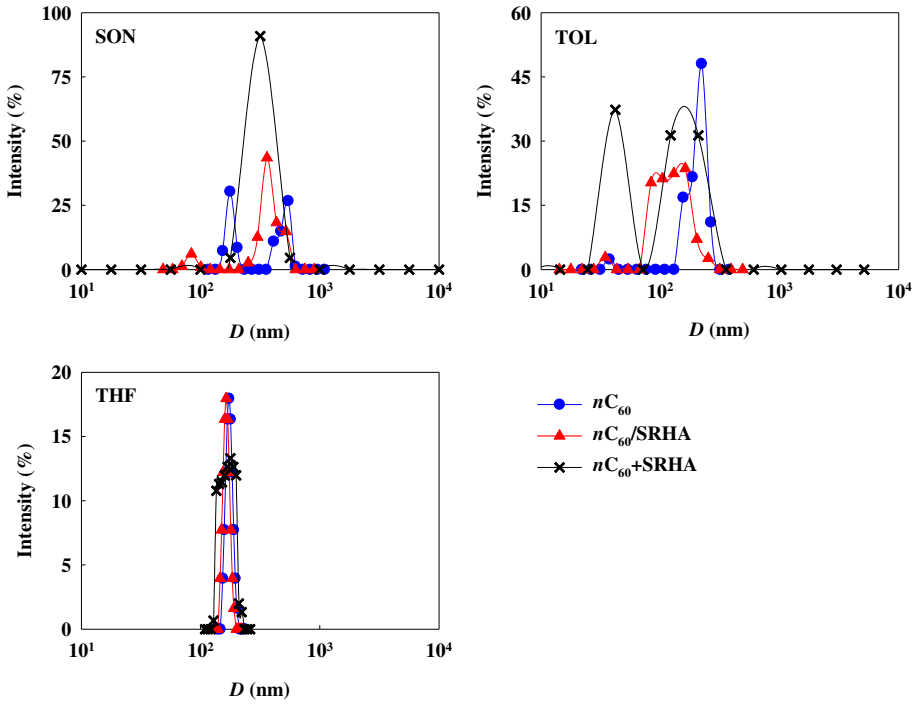

Fig. 1 – Intensity-weighted particle size distribution of different nC_{60} samples. The acronyms "SON", "TOL" and "THF" indicate preparation methods, *i.e.*, sonication, solvent exchange from toluene, and solvent exchange from tetrahydrofuran. The term "nC_{60}" indicates samples prepared in the absence of Suwannee River humic acid (SRHA), and the terms "nC_{60}/SRHA" and "nC_{60} + SRHA" indicate the SRHA-modified samples, for which SRHA was added during or after nC_{60} was formed.

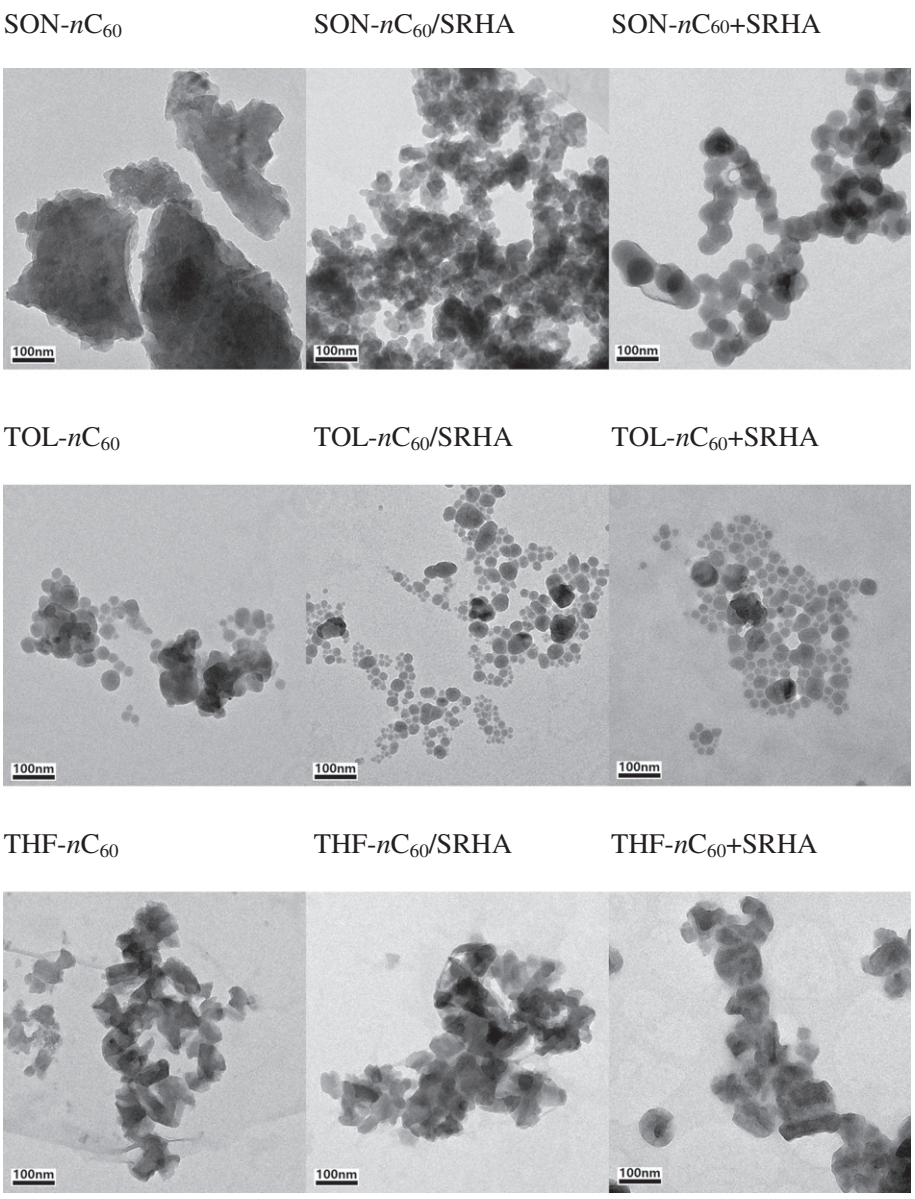

Fig. 2 – Transmission electron microscope (TEM) images of the nC_{60} samples. The acronyms "SON", "TOL" and "THF" indicate preparation methods, *i.e.*, sonication, solvent exchange from toluene, and solvent exchange from tetrahydrofuran. The term "nC_{60}" indicates samples prepared in the absence of Suwannee River humic acid (SRHA), and the terms "nC_{60}/SRHA" and "nC_{60} + SRHA" indicate the SRHA-modified samples, for which SRHA was added during or after nC_{60} was formed.

micrographs in Fig. 2 further corroborate the aforementioned effects of SRHA modification, in that SRHA significantly altered the morphology of the nC_{60} samples synthesized *via* sonication, but had smaller effects on the nC_{60} samples synthesized through solvent exchange.

The UV/vis spectra of nC_{60} samples (Appendix A Fig. S2) show that nC_{60} samples formed *via* different routes had absorption maxima of markedly different shape and position. However, for a given formation route, SRHA modification had little effect on the absorption maximum. These observations were consistent with those reported by others in the literature (Chang and Vikesland, 2011; Wang et al., 2012). All nC_{60} samples were negatively charged, as indicated by the ζ potential values (Table 1). Formation routes and SRHA modification had noticeable effects on ζ potential; however, no clear trend can be established with these data sets.

2.2. Effects of formation routes on adsorption affinities of nC_{60}

The adsorption isotherms of TeCB to the three nC_{60} samples prepared *via* different routes (in the absence of SRHA) are compared in Fig. 3. The isotherms are also shown in logarithm scale (Appendix A Fig. S3) so that differences for low concentration ranges can be seen clearly. Adsorption data were fitted with the Freundlich model: $q = K_F \cdot C^n$, where q (mmol/kg) and C (mmol/L) are the equilibrium concentrations of TeCB on nC_{60} and in the solution, respectively; K_F ($(mmol^{1-n}L^n)/kg$) is the Freundlich affinity coefficient; and n (unitless) is the Freundlich

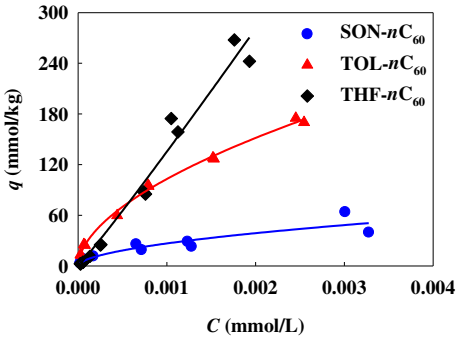

Fig. 3 – Adsorption isotherms of 1,2,4,5-tetrachlorobenzene to nC_{60} samples formed *via* different routes (in the absence of SRHA). The acronyms "SON", "TOL" and "THF" indicate preparation methods, *i.e.*, sonication, solvent exchange from toluene, and solvent exchange from tetrahydrofuran.

linearity index. In general, the Freundlich model fits the adsorption data reasonably well (the fitting parameters are given in Table 1). Interestingly, the adsorption isotherms for SON-nC_{60} and TOL-nC_{60} are considerably more nonlinear compared with that to THF-nC_{60}, indicating higher degrees of heterogeneity in the distribution of adsorption sites. This is consistent with the particle distribution data of the samples (Fig. 1), which shows that THF-nC_{60} was much more uniform in size than SON-nC_{60} and TOL-nC_{60}.

Remarkably, the three nC_{60} samples formed *via* different routes showed significantly different adsorption affinities for TeCB (Fig. 3 and Appendix A Fig. S3). Over the concentration ranges of TeCB studied, the adsorption affinity of TOL-nC_{60} was consistently greater than that of SON-nC_{60}. These differences are primarily attributed to the smaller particle sizes of TOL-nC_{60}, which rendered larger amounts of sites available for adsorption (Cheng et al., 2004; Gai et al., 2011), even though hindered adsorption affinity of SON-nC_{60} due to partial oxidation of C_{60} aggregates during sonication (Murdianti et al., 2012)—which can lower the hydrophobicity of C_{60} aggregates—should not be ruled out. Interestingly, the adsorption affinity of THF-nC_{60} (with the smallest particle size among the three samples) was very low at low TeCB concentrations (slightly lower than that of SON-nC_{60} but approximately an order of magnitude lower than that of TOL-nC_{60}; Appendix A Fig. S3), but increased drastically with increasing TeCB concentration. At the equilibrium TeCB concentration of 0.0006 mmol/L, the adsorption affinity of THF-nC_{60} exceeded that of TOL-nC_{60} (Appendix A Fig. S3). If particle size were the only parameter affecting adsorption sites, then THF-nC_{60}—with the smallest particle size among the three samples—should have had higher adsorption affinity than TOL-nC_{60} and SON-nC_{60} consistently. The concentration-dependent adsorption affinity of THF-nC_{60} appears to be in line with the critical role of pore properties in adsorption of nonionic, hydrophobic organic molecules. As mentioned before (Section 2.1), aggregates of THF-nC_{60} were highly crystalline (tightly packed) and thus had the smallest pore spaces (and possibly a greater amount of closed pores) among the three nC_{60} samples. Since the pore spaces are preferential adsorption sites due to the pore-filling effects (Yang and Xing, 2010), at very low adsorbate concentrations, both TOL-nC_{60} and SON-nC_{60} were stronger adsorbents than THF-nC_{60}. However, the pore spaces can be filled gradually with the increasing mass of adsorbate. Accordingly, at higher TeCB concentrations the differences among the three nC_{60} samples were controlled mainly by the differences in their particle sizes (*i.e.*, available adsorption sites).

2.3. Effects of SRHA modification on adsorption affinities of nC_{60}

The effects of SRHA modification on the adsorption affinities of nC_{60} samples for TeCB are shown in Fig. 4 (the fitted Freundlich model parameters and the distribution coefficients (K_d) are given in Table 1). Note that the q values of the SRHA-modified nC_{60} samples are calculated based on the mass of nC_{60}, rather than the total mass of nC_{60} and SRHA. This was because TeCB adsorption to SRHA was negligible compared to that to nC_{60} (the partition coefficient, K_d, of TeCB to SRHA is $10^{2.02}$, far smaller than the K_d values to nC_{60}, from $10^{4.08}$ to $10^{5.68}$). Interestingly, the effects of SRHA modification varied significantly among the nC_{60} samples formed through different routes.

For the nC_{60} samples prepared by sonication, SRHA modification enhanced adsorption affinities consistently, both when present during the formation of nC_{60} and when added afterward (Fig. 4). Between the two modification approaches, introducing SRHA during sonication had a greater effect in enhancing the adsorption affinities of nC_{60} (Fig. 4). As discussed earlier (Section 2.1), sonication breaks large C_{60} aggregates into smaller ones, and the presence of SRHA in aqueous solution can prevent the re-aggregation of C_{60} aggregates by serving as a stabilizing agent (Chen and Elimelech, 2007; Xie et al., 2008); even when added after sonication, SRHA can still disperse loosely packed C_{60} aggregates. Consequently, the SRHA-modified C_{60} samples (*i.e.*, SON-nC_{60}/SRHA and SON-nC_{60} + SRHA) were much better dispersed and smaller in size compared with the unmodified one (SON-nC_{60}), and had larger amounts of exposed adsorption sites. Since more effective dispersion was achieved when SRHA was present during the sonication, greater adsorption enhancement was observed for SON-nC_{60}/SRHA.

For nC_{60} samples prepared through solvent exchange from toluene, the two SRHA modification methods had opposite effects on the adsorption affinity of nC_{60}: when SRHA was present during phase transfer (*i.e.*, TOL-nC_{60}/SRHA), SRHA modification enhanced the adsorption affinity of nC_{60} noticeably, whereas when added after phase transfer, SRHA modification decreased the adsorption affinity of nC_{60} (Fig. 4). As a "bottom-up" process, phase transfer of C_{60} from toluene to water involved aggregate formation of C_{60} due to a sudden transition from a favorable environment (*i.e.*, toluene, with smaller amount of energy required for cavity formation (Schwarzenbach et al., 2003)) to a highly unfavorable environment (*i.e.*, water, with high-energy required to form cavities, due to the extremely high hydrophobicity of C_{60}). It has been proposed that because toluene is immiscible with water, C_{60} first forms crystal-like primary aggregates and then primary aggregates further form secondary aggregate structures (Martin et al., 1993; Andrievsky et al., 2002; Avdeev et al., 2004; Brant et al., 2006; Chen and Elimelech, 2006). The presence of SRHA in water can facilitate the phase transfer of C_{60} by forming a coating on the primary and secondary

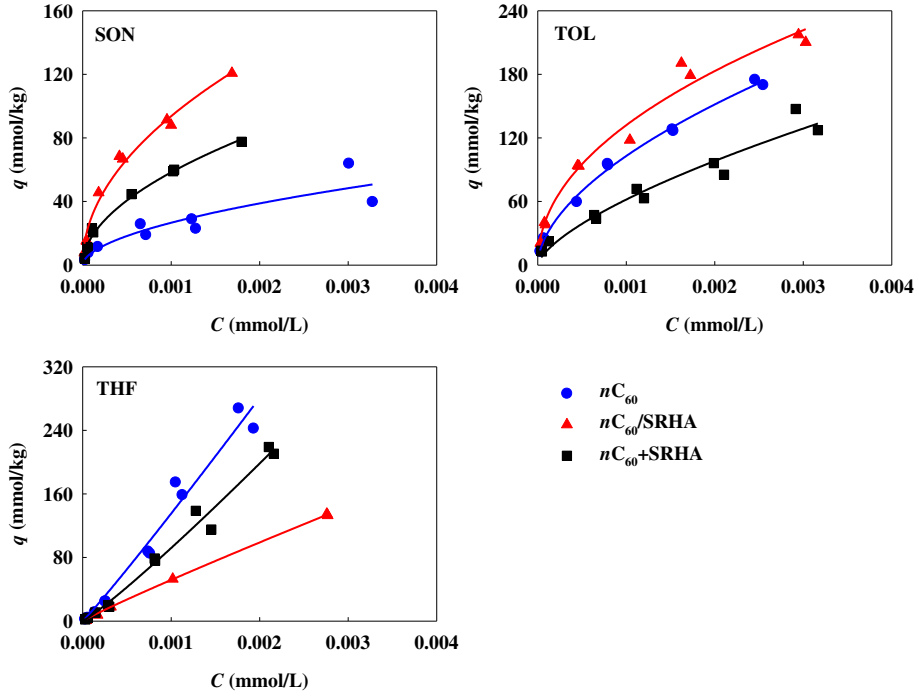

Fig. 4 – Effect of SRHA modification on the adsorption affinities of nC_{60} formed *via* different routes. The acronyms "SON", "TOL" and "THF" indicate preparation methods, *i.e.*, sonication, solvent exchange from toluene, and solvent exchange from tetrahydrofuran. The term "nC_{60}" indicates samples prepared in the absence of Suwannee River humic acid (SRHA), and the terms "nC_{60}/SRHA" and "nC_{60} + SRHA" indicate the SRHA-modified samples, for which SRHA was added during or after nC_{60} was formed.

aggregates. As a result, TOL-nC_{60}/SRHA had smaller particle size than TOL-nC_{60} (Table 1 and Fig. 1) and consequently, greater adsorption affinity. Further, it has been proposed that NOM may serve as a "core" to facilitate the formation of secondary aggregates (Wang et al., 2012). This can make the resulting aggregates relatively less tightly packed and thus more porous, which would favor adsorption of TeCB molecules. Note that unlike the nC_{60} samples formed *via* sonication, the samples formed *via* solvent exchange (in the absence of NOM) are much more tightly packed and thus, adding SRHA after the formation of nC_{60} had very little effect on the aggregation properties of nC_{60}. More importantly, when added after the formation of nC_{60} (*i.e.*, TOL-nC_{60} + SRHA), SRHA likely would coat the surface of the nC_{60} aggregates, and accordingly, would inhibit the adsorption of TeCB by occupying available adsorption sites, and possibly by blocking pore spaces (the high-energy, favorable adsorption sites).

For nC_{60} samples prepared by solvent exchange *via* THF, SRHA modification decreased the adsorption affinity of nC_{60}, especially when SRHA was present during the formation of nC_{60} (Fig. 4). The strikingly inconsistent effects of SRHA modification on the THF-nC_{60} samples compared with the TOL-nC_{60} samples are counter-intuitive, as both approaches involved the phase transfer of C_{60} molecules from a favorable solvent to unfavorable solvent. Here we propose that the differential effects of SRHA were likely due to the fact that THF is a water-miscible solvent whereas toluene is a non-water-miscible solvent. When toluene (containing dissolved C_{60} molecules) was first added to water, it likely existed as small droplets and then gradually evaporated; this was possibly the cause for the formation of primary aggregates. Thus, even when SRHA was present in the aqueous solution, it was likely that SRHA could only coat the primary aggregates, but not C_{60} monomers. However, when THF was added to water, it would immediately mix with water, thus allowing SRHA to interact with (or coat) C_{60} monomers. Consequently, the most prominent effects of SRHA modification on nC_{60} samples formed by solvent exchange from THF was the coating of SRHA on C_{60}, and, a more thorough coating would occur when SRHA was present during the phase transfer. Since SRHA had little effect on particle size when THF was used (Table 1 and Fig. 1), SRHA consistently inhibited the adsorption affinity of nC_{60} by covering adsorption sites, especially when added during the formation of aggregates.

3. Conclusions

The adsorption affinity of nC_{60} for nonionic, hydrophobic 1,2,4,5-tetrachlorobenzene is directly affected by the formation route/processing of nC_{60}, in that the formation route significantly affects the aggregation properties of nC_{60}, which in turn affects the available surface area for adsorption and the extent of adsorption *via* the pore-filling mechanism. The effects of SRHA modification on the adsorption affinity of nC_{60} also vary remarkably depending on the formation route of nC_{60}. Depending on whether nC_{60} is formed *via* the "top-down" route or "bottom-up" route and what kind of solvent is involved, SRHA modification can both enhance and inhibit adsorption affinity of nC_{60}. These findings further demonstrate the complex mechanisms controlling the interactions between

nC_{60} and organic contaminants, and may have significant implications for the life-cycle assessment and holistic environmental risk analysis of C_{60}.

Acknowledgments

This work was supported by the Ministry of Science and Technology (No. 2014CB932001), and the National Natural Science Foundation of China (Nos. 21237002 and 21425729).

Appendix A. Supplementary data

Supplementary data to this article can be found online at http://dx.doi.org/10.1016/j.jes.2016.07.009.

REFERENCES

Andrievsky, G.V., Kosevich, M.V., Vovk, O.M., Shelkovsky, V.S., Vashchenko, L.A., 1995. On the production of an aqueous colloidal solution of fullerenes. J. Chem. Soc. Chem. Commun. 12, 1281–1282.

Andrievsky, G.V., Klochkov, V.K., Bordyuh, A.B., Dovbeshko, G.I., 2002. Comparative analysis of two aqueous-colloidal solutions of C_{60} fullerene with help of FTIR reflectance and UV–Vis spectroscopy. Chem. Phys. Lett. 364, 8–17.

Avdeev, M.V., Khokhryakov, A.A., Tropin, T.V., Andrievsky, G.V., Klochkov, V.K., Derevyanchenko, L.I., Rosta, L., Garamus, V.M., Priezzhev, V.B., Korobov, M.V., Aksenov, V.L., 2004. Structural features of molecular-colloidal solutions of C_{60} fullerenes in water by small-angle neutron scattering. Langmuir 20, 4363–4368.

Brant, J., Lecoanet, H., Wiesner, M.R., 2005. Aggregation and deposition characteristics of fullerene nanoparticles in aqueous systems. J. Nanopart. Res. 7, 545–553.

Brant, J.A., Labille, J., Bottero, J.Y., Wiesner, M.R., 2006. Characterizing the impact of preparation method on fullerene cluster structure and chemistry. Langmuir 22, 3878–3885.

Campoy-Quiles, M., Ferenczi, T., Agostinelli, T., Etchegoin, P.G., Kim, Y., Anthopoulos, T.D., Stavrinou, P.N., Bradley, D.D., Nelson, J., 2008. Morphology evolution via self-organization and lateral and vertical diffusion in polymer: fullerene solar cell blends. Nat. Mater. 7, 158–164.

Chang, X., Vikesland, P.J., 2009. Effects of carboxylic acids on nC_{60} aggregate formation. Environ. Pollut. 157, 1072–1080.

Chang, X., Vikesland, P.J., 2011. UV–vis spectroscopic properties of nC_{60} produced via extended mixing. Environ. Sci. Technol. 45, 9967–9974.

Chang, X., Duncan, L.K., Jinschek, J., Vikesland, P.J., 2012. Alteration of nC_{60} in the presence of environmentally relevant carboxylates. Langmuir 28, 7622–7630.

Chen, K.L., Elimelech, M., 2006. Aggregation and deposition kinetics of fullerene (C_{60}) nanoparticles. Langmuir 22, 10994–11001.

Chen, K.L., Elimelech, M., 2007. Influence of humic acid on the aggregation kinetics of fullerene (C_{60}) nanoparticles in monovalent and divalent electrolyte solutions. J. Colloid Interface Sci. 309, 126–134.

Cheng, X., Kan, A.T., Tomson, M.B., 2004. Naphthalene adsorption and desorption from aqueous C_{60} fullerene. J. Chem. Eng. Data 49, 675–683.

Cheng, X., Kan, A.T., Tomson, M.B., 2005. Uptake and sequestration of naphthalene and 1,2-dichlorobenzene by C_{60}. J. Nanopart. Res. 7, 555–567.

Duncan, L.K., Jinschek, J.R., Vikesland, P.J., 2008. C_{60} colloid formation in aqueous systems: effects of preparation method on size, structure, and surface charge. Environ. Sci. Technol. 42, 173–178.

Fortner, J.D., Lyon, D.Y., Sayes, C.M., Boyd, A.M., Falkner, J.C., Hotze, E.M., Alemany, L.B., Tao, Y.J., Guo, W., Ausman, K.D., Colvin, V.L., Hughes, J.B., 2005. C_{60} in water: nanocrystal formation and microbial response. Environ. Sci. Technol. 39, 4307–4316.

Gai, K., Shi, B., Yan, X., Wang, D., 2011. Effect of dispersion on adsorption of atrazine by aqueous suspensions of fullerenes. Environ. Sci. Technol. 45, 5959–5965.

Henry, T.B., Menn, F.M., Fleming, J.T., Wilgus, J., Compton, R.N., Sayler, G.S., 2007. Attributing effects of aqueous C_{60} nano-aggregates to tetrahydrofuran decomposition products in larval zebrafish by assessment of gene expression. Environ. Health Perspect. 115, 1059–1065.

Hu, X., Liu, J., Mayer, P., Jiang, G., 2008. Impacts of some environmentally relevant parameters on the sorption of polycyclic aromatic hydrocarbons to aqueous suspensions of fullerene. Environ. Toxicol. Chem. 27, 1868–1874.

Hüffer, T., Kah, M., Hofmann, T., Schmidt, T.C., 2013. How redox conditions and irradiation affect sorption of PAHs by dispersed fullerenes (nC_{60}). Environ. Sci. Technol. 47, 6935–6942.

Hwang, Y.S., Li, Q., 2010. Characterizing photochemical transformation of aqueous nC_{60} under environmentally relevant conditions. Environ. Sci. Technol. 44, 3008–3013.

Klaine, S.J., Alvarez, P.J.J., Batley, G.E., Fernandes, T.F., Handy, R.D., Lyon, D.Y., Mahendra, S., McLaughlin, M.J., Lead, J.R., 2008. Nanomaterials in the environment: behavior, fate, bioavailability, and effects. Environ. Toxicol. Chem. 27, 1825–1851.

Li, D., Lyon, D.Y., Li, Q., Alvarez, P.J.J., 2008. Effect of soil sorption and aquatic natural organic matter on the antibacterial activity of a fullerene water suspension. Environ. Toxicol. Chem. 27, 1888–1894.

Li, Q., Xie, B., Hwang, Y.S., Xu, Y., 2009. Kinetics of C_{60} fullerene dispersion in water enhanced by natural organic matter and sunlight. Environ. Sci. Technol. 43, 3574–3579.

Martin, T.P., Naher, U., Schaber, H., Zimmermann, U., 1993. Clusters of fullerene molecules. Phys. Rev. Lett. 70, 3079–3082.

Mauter, M.S., Elimelech, M., 2008. Environmental applications of carbon-based nanomaterials. Environ. Sci. Technol. 42, 5843–5859.

Murdianti, B.S., Damron, J.T., Hilburn, M.E., Maples, R.D., Hikkaduwa Koralege, R.S., Kuriyavar, S.I., Ausman, K.D., 2012. C_{60} oxide as a key component of aqueous C_{60} colloidal suspensions. Environ. Sci. Technol. 46, 7446–7453.

Qu, X., Hwang, Y.S., Alvarez, P.J.J., Bouchard, D., Li, Q., 2010. UV irradiation and humic acid mediate aggregation of aqueous fullerene (nC_{60}) nanoparticles. Environ. Sci. Technol. 44, 7821–7826.

Sayes, C.M., Fortner, J.D., Guo, W., Lyon, D., Boyd, A.M., Ausman, K.D., Tao, Y.J., Sitharaman, B., Wilson, L.J., Huges, J.B., West, J.L., Colvin, V.L., 2004. The differential cytotoxicity of water-soluble fullerenes. Nano Lett. 4, 1881–1887.

Schwarzenbach, R.P., Gschwend, P.M., Imboden, D.M., 2003. Environmental Organic Chemistry. second ed. Wiley-InterScience, New York.

Simon, F., Peterlik, H., Pfeiffer, R., Bernardi, J., Kuzmany, H., 2007. Fullerene release from the inside of carbon nanotubes: a possible route toward drug delivery. Chem. Phys. Lett. 445, 288–292.

Wang, L., Huang, Y., Kan, A.T., Tomson, M.B., Chen, W., 2012. Enhanced transport of 2,2′,5,5′-polychlorinated biphenyl by natural organic matter (NOM) and surfactant-modified fullerene nanoparticles (nC_{60}). Environ. Sci. Technol. 46, 5422–5429.

Wang, L., Hou, L., Wang, X., Chen, W., 2014. Effects of the preparation method and humic-acid modification on the

mobility and contaminant-mobilizing capability of fullerene nanoparticles (nC_{60}). Environ. Sci. Process Impacts. 16, 1282–1289.

Xie, B., Xu, Z., Guo, W., Li, Q., 2008. Impact of natural organic matter on the physicochemical properties of aqueous C_{60} nanoparticles. Environ. Sci. Technol. 42, 2853–2859.

Yang, K., Xing, B., 2007. Desorption of polycyclic aromatic hydrocarbons from carbon nanomaterials in water. Environ. Pollut. 145, 529–537.

Yang, K., Xing, B., 2010. Adsorption of organic compounds by carbon nanomaterials in aqueous phase: Polanyi theory and its application. Chem. Rev. 110, 5989–6008.

Yang, K., Zhu, L., Xing, B., 2006. Adsorption of polycyclic aromatic hydrocarbons by carbon nanomaterials. Environ. Sci. Technol. 40, 1855–1861.

Zhang, L., Wang, L., Zhang, P., Kan, A.T., Chen, W., Tomson, M.B., 2011. Facilitated transport of 2,2′,5,5′-polychlorinated biphenyl and phenanthrene by fullerene nanoparticles through sandy soil columns. Environ. Sci. Technol. 45, 1341–1348.